NASA
Technical Memorandum 100559

USAAVSCOM
Technical Memorandum 88-B-001

A Preliminary Investigation of Finite-Element Modeling for Composite Rotor Blades

Renee C. Lake and Mark W. Nixon

January 1988

NASA

National Aeronautics and
Space Administration

Langley Research Center
Hampton, Virginia 23665

United States Army
Aviation Systems
Command

Aviation R&T Activity

A Preliminary Investigation of Finite-Element
Modeling for Composite Rotor Blades

Renee C. Lake and Mark W. Nixon
Aerostructures Directorate
U. S. Army Aviation Research and Technology Activity - AVSCOM
NASA Langley Research Center
Hampton, Virginia 23665-5225

Abstract

The results from an initial phase of an in-house study aimed at improving the dynamic and aerodynamic characteristics of composite rotor blades through the use of elastic couplings are presented. Large degree-of-freedom shell-finite-element models of an extension-twist-coupled composite tube were developed and analyzed using MSC/NASTRAN. An analysis employing a simplified beam finite-element representation of the specimen with the equivalent engineering stiffnesses (equivalent-beam analysis) was additionally performed. Results from the shell-finite-element normal modes and frequency analysis were compared to those obtained experimentally, showing agreement within 13%. In addition, a comparison with results from the equivalent-beam analysis indicated that, although the analysis accurately predicted frequencies for the bending modes, which are essentially uncoupled, there was an appreciable degradation in the frequency prediction for the torsional mode, which is elastically-coupled. This was due to the absence of off-diagonal coupling terms in the formulation of the equivalent engineering stiffnesses. Parametric studies of frequency variation due to small changes in ply orientation angle and ply thickness were also performed. Results showed linear frequency variations less than 2.0% per 1° variation in the ply orientation angle, and 1% per 0.0001 inch variation in the ply thickness.

Nomenclature

A beam cross-sectional area, in^2

$B_{y,x}$ beam curvature (flapwise), in^{-1}

$B_{z,x}$ beam curvature (chordwise), in^{-1}

C_{ij} coupled-beam stiffness terms (from ref. 9)

E extension modulus, psi

EA beam uncoupled extensional stiffness, lb

EI_c beam uncoupled bending stiffness (chordwise), $lb\text{-}in^2$

EI_f beam uncoupled bending stiffness (flapwise), $lb\text{-}in^2$

G shear modulus, psi

GK beam uncoupled torsional stiffness, $lb\text{-}in^2$

I_c beam area moment of inertia (chordwise), in^4

I_f beam area moment of inertia (flapwise), in^4

K beam torsional constant, in^4

M_x beam torsional moment, $in\text{-}lb$

M_y beam bending moment (flapwise), $in\text{-}lb$

M_z beam bending moment (chordwise), $in\text{-}lb$

N_x beam axial force, lb

Q_y beam shear (chordwise), lb

Q_z beam shear (flapwise), lb

S_{ij} coupled-beam compliance terms (from ref. 9)

t lamina thickness, in

$U_{,x}$ beam extensional strain

$V_{,x}$ beam shear strain (chordwise)

$W_{,x}$ beam shear strain (flapwise)

θ ply orientation angle, deg

ν Poisson ratio

$\phi_{,x}$ beam twist rate, deg/in

1,2,12   principle directions

Introduction

Advancements in composite material technology have spurred the increased use of composites in modern rotorcraft structures. In addition to the desirable high-strength, low-weight features of these materials, the potential for elastic tailoring of the structural properties has made composites particularly attractive for advanced structural applications. Currently, attention is being focused on the use of composite materials for designing rotor blades in which the elastic coupling associated with unbalanced ply layup is employed to enhance the dynamic and aerodynamic characteristics. Other useful applications of elastic coupling include the reduction or modification of structural vibration in rotor blade design. The ability to analytically predict the dynamic characteristics of elastically-coupled composite rotor blades is essential to these applications. However, due to the complex, directional nature of composite materials, the analysis of anisotropically-laminated structures is complicated by the introduction of elastic couplings. This is notably true of the structural dynamic behavior, because the elastic couplings can have a significant influence on the dynamic characteristics, such as mode shape and frequency. Thus, there is a need for improved and verified dynamic analyses which account for elastic couplings.

The analysis of helicopter rotor blades has traditionally depended upon classical shell or beam theory-based analyses, which are provided by various sources in the literature. Analyses based on classical shell theory (refs. 1 - 3, for example) have generally examined the dynamic characteristics of orthotropic and anisotropically-laminated cylindrical shells, which can be thought of as rudimentary rotor blade structures. These analyses, however, do not readily lend themselves to
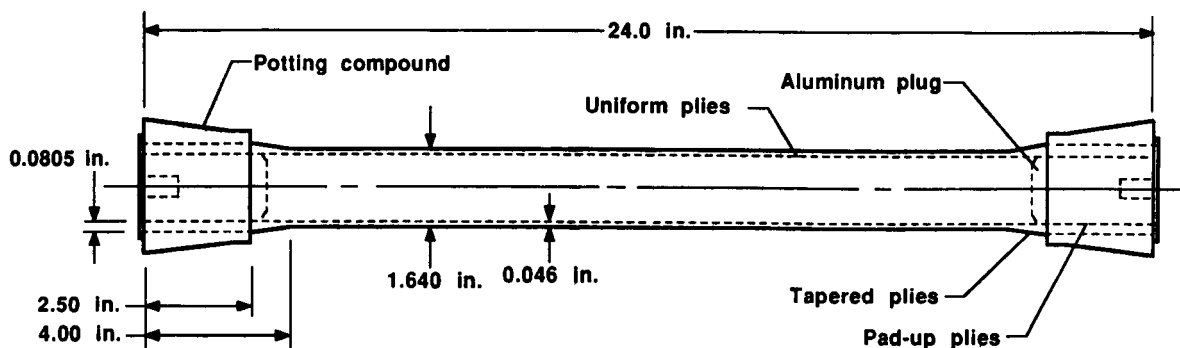
Fig. 1 - Sectional view of T300/5208 Gr/E tube

existing dynamic and aeroelastic stability codes, which generally employ beam-like structural representations of the rotor blades. Structural analyses which use equivalent beam element formulations have received considerable attention in the literature (refs. 4 - 6). These analyses are desirable from a preliminary or basic design viewpoint because of reduced computational overhead, ease of model definition and interpretation, and compatibility with existing aeroelastic codes. Other treatments of beam representations for anisotropically-laminated rotor blade structures are found in various beam theories (refs. 7 - 9, for example). While analyses based on beam-like representations are generally feasible methods of structural analyses for many composite rotor blade structures, the design of advanced rotor blades will often require a more rigorous and comprehensive analytical representation, such as that embodied by a detailed shell-finite-element representation.

Finite-element analysis has become an established and widely implemented tool in the design of rotorcraft airframes. Recently, however, research efforts have indicated a growing interest in applying finite-element analysis techniques in composite rotor blade structural analyses. In addition to multipurpose finite-element codes which possess composite material capability (refs. 10 - 15), additional composite plate and shell finite-elements have been formulated by various investigators. For example, numerous research efforts have focused on the development of shell elements with anisotropic laminate capabilities (refs. 16, 17, 18). Furthermore, advancements in element formulation, including thick-plate capability (ref. 19), and higher-order elements (ref. 20) have been investigated. While these examples illustrate the successful implementation of the finite-element method in various composite material structural analyses, technology transfer is not facilitated through the use of specialized codes. For this reason, it is desirable to investigate the advanced capabilities of widely-implemented, commercially-available finite-element codes. MSC/NASTRAN was selected as the baseline analytical code for this investigation because it is the primary structural analysis tool used by the rotorcraft industry, and technology transfer could best be promoted through its use.

The purpose of this paper is to present results from an initial phase of an in-house study aimed at improving the dynamic and aerodynamic characteristics of rotor blades through the use of elastic couplings. Extension-twist elastic coupling, which exhibits coupling among the extensional and torsional stiffnesses of a structure, was studied in this investigation. Potential applications of extension-twist coupling include the design of a tilt-rotor blade that would change twist as a function of rotor speed. To this end, a study was initiated in which dynamic results from large degree-of-freedom shell-finite-element models were correlated with experimental results obtained from a vibration test of an extension-twist-coupled composite tube specimen. In addition, the results were compared with those obtained from a simplified beam-finite-element representation of the specimen. This comparison was performed to establish the range of applicability of the simpler beam analysis. Because the beam model was given equivalent engineering stiffnesses which did not include the coupling effects present in the shell-finite-element model, the effects of neglecting the elastic-coupling stiffnesses could be determined. Studies aimed at assessing the influence of small parametric variations in structural properties on the predicted natural frequencies were additionally performed. The ply orientation angle and the ply thickness were selected as the parametric variables for these studies.

Description of Composite Tube Specimen

The specimen which was tested and analyzed was an extension-twist-coupled circular tube (see fig. 1). The tube was fabricated from uni-directional T300/5208 graphite fiber/epoxy resin (0.00575 inch measured thickness per ply), with a $[(+20^\circ/-70^\circ)_2]_s$ layup (see Table I for material properties). The specimen was circular in cross section with a 1.640 inch outside diameter and a 0.046 inch wall thickness. Because the tube specimen was prepared for static testing purposes prior to the dynamic test, additional features were permanently incorporated into the design to facilitate static testing.

2

Table 1 - T300/5208 Gr/E orthotropic
material properties

E_{11}	23.10 E6	psi
E_{22}	1.38 E6	psi
G_{12}	0.73 E6	psi
ν_{12}	0.38	

- 722 Grid points
- 684 CQUAD4 plate elements
- 174 Total dynamic degrees
  of freedom

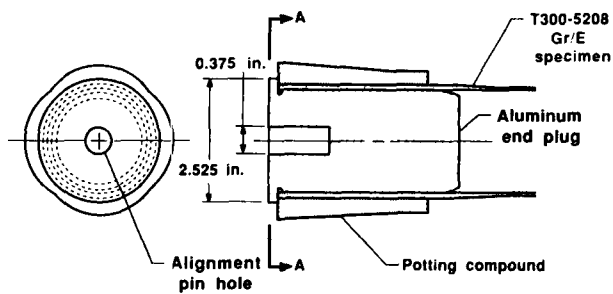Fig. 3 - "Built-up" finite-element model of tube

Fig. 2 - Sectional view of specimen end design

Additional "pad-up" plies were added in step-wise fashion
to each end of the specimen to avoid end load stress con-
centrations induced by the tensile test fixture. Attachment
to the test fixture was facilitated by molding a potting com-
pound (TC-5467+ resin with HD-0111+ hardener) to each
end of the specimen. In addition, an aluminum plug was in-
serted into each end of the specimen to prevent cross-sectional
crushing deformation. Details of the end design features are
illustrated in figure 2. These structural features were a per-
manent feature of the specimen and could not be removed for
the vibration test. Thus, the corresponding mass and stiff-
ness properties of the end plug and potting compound were
included in the finite-element model.

Description of Finite-Element Models

The composite tube was modeled and analyzed using the
MSC/NASTRAN (refs. 10 - 13) finite-element program as
the baseline analysis tool. The body of the tube was modeled
using two-dimensional, quadrilateral flat plate elements which
have anisotropic properties (fig. 3). A lumped-mass represen-
tation was employed for the associated structural mass. The
built-up finite-element models had a total of 722 grid points
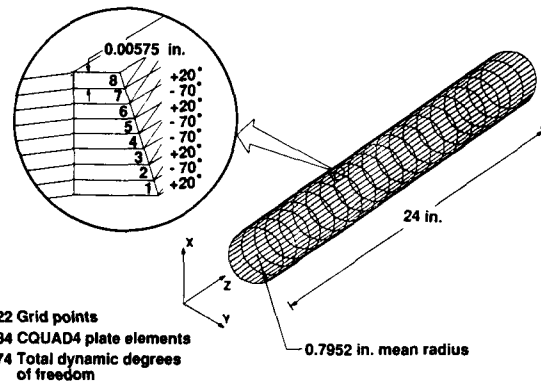(each having three translational and three rotational degrees

of freedom), 684 plate (CQUAD4) elements, and 174 dynamic
degrees of freedom (obtained through static condensation).
Concentrated mass (CONM2) elements were used for mod-
eling the potting compound and aluminum end plugs (non-
structural mass). In addition, the end plugs were assumed
rigid and were therefore modeled with rigid (RBE2) elements.
The plane of grid points coincided with the center of the lam-
inate (reference plane). Therefore, the cross-sectional radius
indicated in figure 3 is a measurement of this distance.

Five different finite-element models were developed for dy-
namic analyses. Of these, four models were developed to study
the effect of non-structural mass representation. The four
models shared the same basic structure (as described above).
The fifth model was a simplified version of the former models,
and was used for parametric studies.

Representation of Non-Structural Mass

The finite-element representation of the non-structural
mass (potting compound and aluminum end plugs) of the
tube was an important modeling consideration. This mass
comprised 88% of the total specimen weight and had a sig-
nificant influence on the dynamic characteristics of the spec-
imen. To determine the optimum modeling configuration for
the actual mass distribution and inertial effects, four sepa-
rate finite-element models were developed. The primary dif-
ference between each model lies in the number and configu-
ration of concentrated mass elements used to represent the
non-structural mass. The details of the mass representation
for the four models are shown in figure 4. (Because of the
structural symmetry, only one end of the tube is depicted).

The first model, DELTA1, had the simplest mass repre-
sentation. The total non-structural mass for each end was di-
vided evenly between each of the 36 grid points of the second
cross-section. This location approximated the axial centroid
of the total mass at each end. Furthermore, each mass was
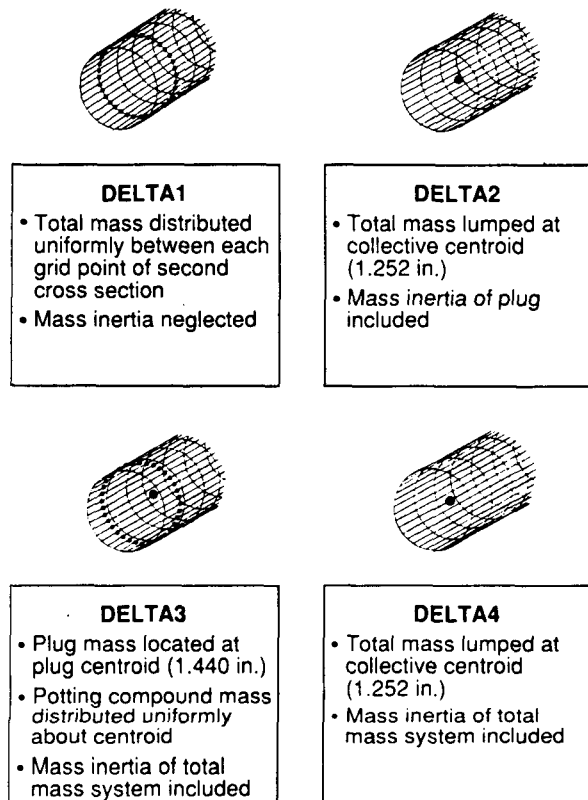considered a point mass with no individual inertia.

3

DELTA1
- Total mass distributed uniformly between each grid point of second cross section
- Mass inertia neglected

DELTA2
- Total mass lumped at collective centroid (1.252 in.)
- Mass inertia of plug included

DELTA3
- Plug mass located at plug centroid (1.440 in.)
- Potting compound mass distributed uniformly about centroid
- Mass inertia of total mass system included

DELTA4
- Total mass lumped at collective centroid (1.252 in.)
- Mass inertia of total mass system included

Fig. 4 - Representation of non-structural mass

0.7952 in. mean radius

24 in.

x

z

y

- 158 Grid points
- 144 CQUAD4 plate elements
- 96 Total dynamic degrees of freedom

Fig. 5 - Simplified finite-element model of tube

DELTA2, the second finite-element model, was an upgrade of the first model with respect to treatment of inertia. The total non-structural mass for each end was collectively modeled with a single concentrated mass element placed at the centroid of the total end mass (1.252 inches from each end of the tube). The effective inertia corresponding to each end plug was accounted for using a solid cylinder approximation, while the effective inertia of each potting compound mass was neglected.

The third mass representation was developed in the DELTA3 finite-element model. The mass of each end plug was modeled with a single concentrated mass element, located at the centroid of each plug (1.440 inches from each end). The inertial effect of each plug was again accounted for using a solid cylinder approximation. The mass of the potting compound (each end) was divided evenly between the grid points of the second cross-section, and was axially offset at the calculated centroid of the potting compound. Each grid point mass was again considered a point mass, with no individual inertia.

The fourth mass representation was developed in the DELTA4 model. The total non-structural mass (end plug plus potting compound) for each end was collectively modeled as a single concentrated mass, at the centroid of each total end mass (1.252 inches from each end of the tube). The corresponding inertias were individually calculated for each end plug and potting compound based on solid cylinder and conical frustum approximations, respectively.
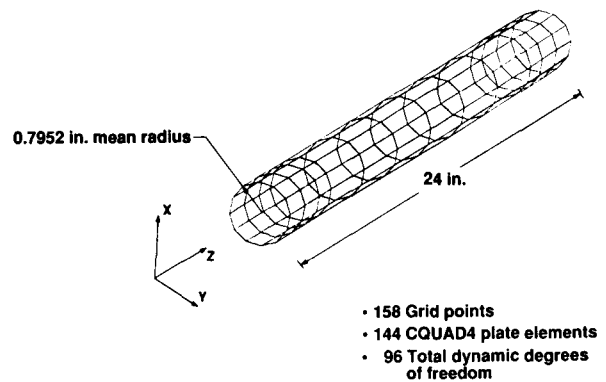
Finite Element Model for Parametric Studies

The finite-element model used for the parametric studies was a simplified derivative of the "built-up" (larger degree-of-freedom) models previously described, and is shown in figure 5. A simplified model was employed in these studies to decrease computer time and costs, and additionally provided an insight into the degree of element mesh size required for accurate results. The total number of grid points and plate elements was reduced to 158 and 144, respectively. The total number of dynamic degrees of freedom was correspondingly decreased to 96. (This represents an 80% reduction in the number of elements, and a 45% decrease in the total number of degrees of freedom.) The non-structural mass (aluminum end plugs and potting compound) of the tube was modeled with single concentrated mass elements placed at each end mass centroid. The methodology for representing the non-structural mass was identical to that used in the DELTA4 finite-element model.

Equivalent-Beam Representation

The effect of equivalent-beam representation on the dynamic characteristics of the composite tube was investigated. The equivalent-beam properties were calculated for the composite tube specimen, based on known geometrical and material characteristics. The equivalent-beam analysis of reference 21 was selected for the beam representation study, because of the excellent correlation with an MSC/NASTRAN shell-finite-element model. The comparison of static displacement results showed very good agreement and established confidence in this equivalent-beam analysis.

The equivalent-beam analysis allows an elastically-coupled composite structure to be described in terms of its equivalent engineering properties (EA, EI, GK). The beam properties are obtained via the closed-form single-cell analysis described in reference 21, which is based on the theory in reference 9. As

shown in reference 21, a fully populated 6 x 6 stiffness matrix $[C_{ij}]$ is calculated for the structure, relating beam forces and deformations:

$$\begin{bmatrix} N_z \\ Q_y \\ Q_z \\ M_z \\ M_y \\ M_z \end{bmatrix} = \begin{bmatrix} C_{ij} \end{bmatrix} \begin{bmatrix} U_{,z} \\ V_{,z} \\ W_{,z} \\ \phi_{,z} \\ B_{y,z} \\ B_{z,z} \end{bmatrix} \tag{1}$$

Because of elastic coupling effects, the equivalent beam stiffnesses are not quantitatively equal to the diagonal terms of the stiffness matrix, but are instead obtained from the compliance matrix $[S_{ij}]$. The compliance matrix relates beam deformations to forces and is simply the inverse of the stiffness matrix:

$$\begin{bmatrix} U_{,z} \\ V_{,z} \\ W_{,z} \\ \phi_{,z} \\ B_{y,z} \\ B_{z,z} \end{bmatrix} = \begin{bmatrix} S_{ij} \end{bmatrix} \begin{bmatrix} N_z \\ Q_y \\ Q_z \\ M_z \\ M_y \\ M_z \end{bmatrix} \tag{2}$$

As shown in reference 21, the equivalent engineering stiffnesses are accurately obtained from the reciprocal of the diagonal terms in the compliance matrix. Therefore, using the following equations:

$$EA = \frac{1}{S_{11}} \tag{3}$$

$$EI_c = \frac{1}{S_{55}} \tag{4}$$

$$EI_f = \frac{1}{S_{66}} \tag{5}$$

$$GK = \frac{1}{S_{44}} \tag{6}$$

the equivalent properties for the structure can be determined, based on the known values of cross-sectional area (A) and torsion constant (K). The equivalent Young's Modulus (E) can be extracted through the division of equation (3) by the known cross-sectional area of the tube (A). This equivalent value of E is then substituted into equations (4) and (5), yielding the equivalent values of the chordwise and flapwise inertias, I_c and I_f, respectively. The equivalent shear modulus (G) is obtained by dividing equation (6) by the known torsional constant (K) of the section. The resulting equivalent values of E, A, and G are subsequently used in a finite-element model of the composite specimen, which uses simple beam elements as the structural components. Table II summarizes the calculated equivalent properties for the three different sections of the composite tube specimen. Values are reported for the pad-up, tapered, and uniform sections, in which the number of plies (and cross-sectional dimensions) varied.

Table II - "Equivalent" isotropic material properties

Section type	E, psi	G, psi	ν
Pad-Up	5.971 E6	3.047 E6	0.38
Tapered	6.159 E6	2.726 E6	0.38
Uniform	5.581 E6	1.403 E6	0.38

Parametric Studies

Due to the possibility of discrepancies in material property data, or the presence of slight structural imperfections in the specimen, a parametric study of frequency variation was desirable. Two parametric variables were chosen for this study: the orientation angle of the plies (θ), and the ply thickness of the material (t). These variables were selected based on the following considerations. The tube was constructed by a hand lay-up method, therefore slight variations in the actual ply orientation angle were realistic to consider. In addition, variations in ply thickness may be a function of curing processes, and may not always agree with actual vendor data.

For the ply orientation angle study, ply angle values were varied about the +20° and -70° baselines for each ply in ±1° increments. This 1° step size was considered a realistic deviation representative of this method of fabrication. The nominal ply thickness and material properties remained unchanged. The ply angle was varied up to a maximum of ±4° about the baseline, spanning a total range of 8°. The cross plies remained mutually normal in the variations (i.e., the 90° included angle was preserved).

The second parametric study involved the variation of frequency with ply thickness. The thickness variation per ply was on the order of 2.0% of the ply thickness, or ±0.0001 inch per ply. The fiber/matrix volume fraction was assumed to remain constant, with no significant changes in material properties. Each ply was assumed to vary uniformly throughout the laminate, with the thickness variation spanning a maximum range of 0.0008 inches.

Vibration Test Setup

The vibration test setup is shown in figure 6. The composite tube specimen was suspended from a fixed structure with bungee cords, simulating a free-free boundary condition. Specimen excitation was performed through a series of prescribed hammer taps. A three-axis accelerometer transducer was mounted on one end of the specimen, at an offset from the center (to aid in torsional frequency determination).

Fig. 6 - Vibration test set-up for Gr/E specimen

Fig. 7 - Results from mass representation study

Results and Discussion

Comparison of Dynamic Results with Test Results

Three natural frequencies (first bending, first torsion, and second bending) were identified from the vibration test. These frequencies were compared with results of the dynamic analyses performed on the four shell-finite-element models, and are shown in figure 7. The first mass representation model, DELTA1, yielded the poorest overall correlation. All frequency values were larger than the experimental values, with first and second bending frequencies varying by 16.0% and 39.0%, respectively. The torsional frequency however, agreed very well with the experimental frequency (within 3.5%). The DELTA2 model showed slightly improved correlation over DELTA1 for the bending cases, but a significant decrease in torsional frequency agreement (44.4%). This is due to the absence of the circumferentially distributed mass of the potting compound in the finite-element model. Consequently, the inertial effect of this mass (due to a radial offset) was not present in the finite-element model, thereby increasing the calculated torsional frequency. The DELTA3 model showed improved overall performance with respect to frequency correlation. First and second bending frequencies agreed within 9.3% and 17.2%, respectively. The torsional frequency was 9.0% higher than the experimental value. The final mass representation, DELTA4, gave the best overall agreement. First and second bending frequencies were in good agreement with experimental values, exhibiting a maximum error of 13.4% (second bending frequency). The torsional frequency was slightly improved (8.9%) over the DELTA3 results, and agreed well with the experimental frequency. Therefore, the DELTA4 finite-element model was selected as the baseline model for the equivalent-beam correlation studies. A plot of the analytical mode shapes is presented in figure 8 for the baseline model. This figure qualitatively illustrates the basic modal deformations of the tube. The exaggerated narrowing of the central region of the tube, as seen in the torsional mode plot, is apparently a function of the NASTRAN plotter and is not to scale.
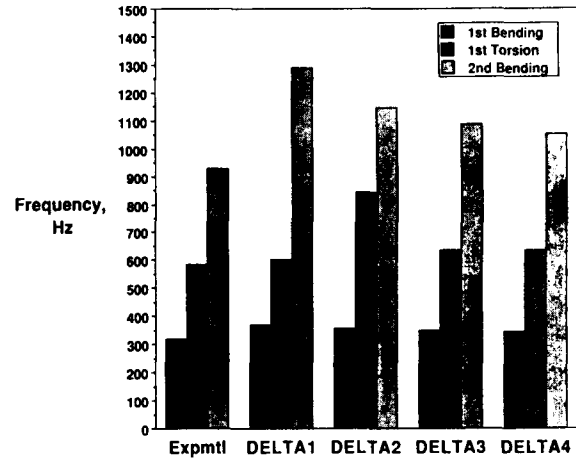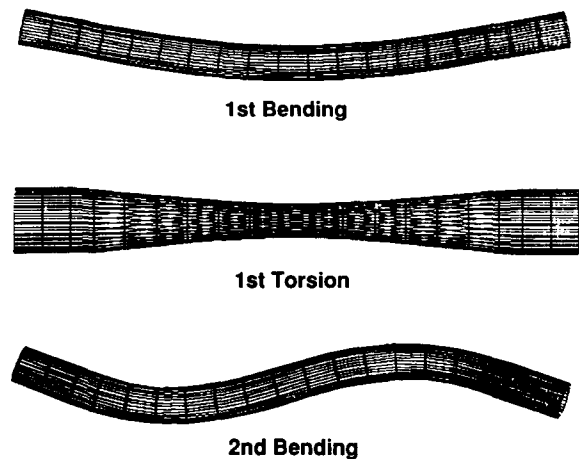

1st Bending

1st Torsion

2nd Bending

Fig. 8 - Mode shapes from finite-element analysis

Comparison of Dynamic Results with Equivalent-Beam Results

Results from a normal modes and frequency analysis for the equivalent-beam finite-element model were compared to those obtained experimentally as well as with the baseline (DELTA4) model and are shown in figure 9. The equivalent-beam first bending frequency agreed very well with the baseline finite-element model frequency (within 1.3%), and was 9.2% higher than the experimental value. A similar trend was observed for the second bending frequencies. Results of the torsional frequency comparison, however, showed a diminished correlation for the equivalent-beam analysis. The predicted equivalent-beam frequency was approximately 14.0% higher than the baseline model and 24.6% higher than the experimental frequency. The degradation in the overall performance of the equivalent-beam analysis is largely due to the absence of the off-diagonal compliance terms in the determination of the equivalent properties. These terms, partic-
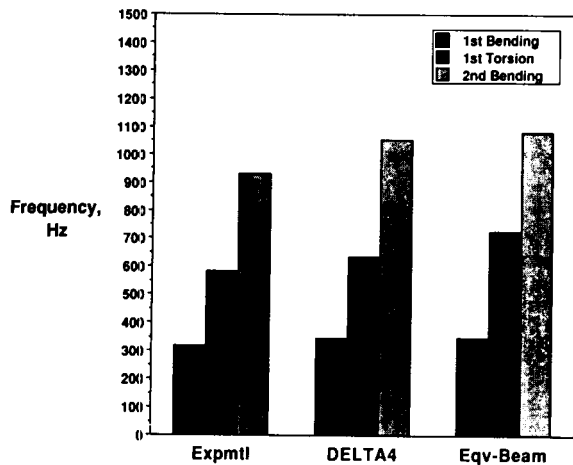
6

Fig. 9 - Comparison of frequencies
for baseline configuration

Fig. 11 - Modal frequency as a function
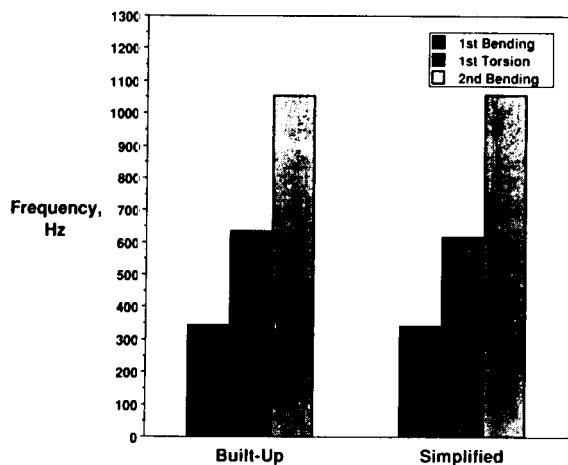of ply orientation angle

Fig. 10 - Effect of baseline model simplification

ularly C_{14} (extension-twist coupling term) quantify the coupling behavior of the structure and are particularly important for modes which are influenced by elastic coupling. Therefore, an appreciable degradation in the prediction accuracy can be expected for the frequencies of such modes when the off-diagonal compliance terms are neglected in the analysis.

Effect of Finite-Element Model Simplification

As mentioned earlier, the basic finite-element model used for the studies was simplified from the "built-up" finite-element models used in the non-structural mass studies. The effect of simplifying the finite-element model is shown in figure 10. A 0.8% decrease in natural frequency was noted for the first bending mode, while the second bending mode frequency in-
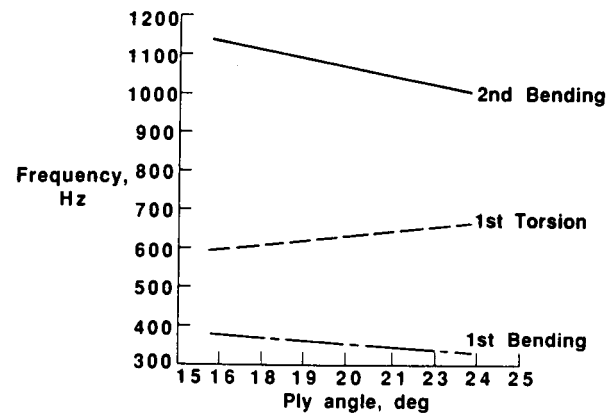
creased by 0.5%. The torsional frequency decreased by 3.0% from that calculated for the built-up model. The simplified model was used as a baseline model in the parametric studies and all variations are calculated from this baseline. The results of this simplification exercise suggest that a strategically-reduced finite-element model (coarser element mesh with corresponding fewer degrees of freedom) can predict frequencies which are in good agreement with those obtained using a more complex model.

Results of Parametric Studies

The results of the ply orientation angle study are shown in figure 11. Frequency was observed to vary approximately linearly with the change in ply angle. The frequencies of the first and second bending modes varied inversely with ply angle producing an average decrement in frequency of 1.9% and 1.7% per 1° increment in ply angle, respectively. This effect is produced by a decrease in the effective axial stiffness with increasing ply angle. The total magnitude of percent frequency change over the 8° range was slightly greater for the first bending mode than the second bending mode (approximately 7.8% versus 6.6%). The torsional frequency, however, was found to vary directly with the change in ply angle, yielding an average increase in frequency of 1.5% per 1° increment in ply angle. This trend is produced by an increase in torsional stiffness, which corresponds to an increase in ply angle (for angles less than 45°).

The results of the ply thickness study are shown in figure 12. The observed variation in frequency with ply thickness was again approximately linear for the range of thickness considered (0.00535 in. - 0.00615 in.). Furthermore, all three frequencies were found to vary directly with ply thickness, although the magnitude per 0.0001 inch variation was greater for the first torsion mode (±0.8%) than for the first and second bending modes (±0.3% and ±0.5%, respectively).
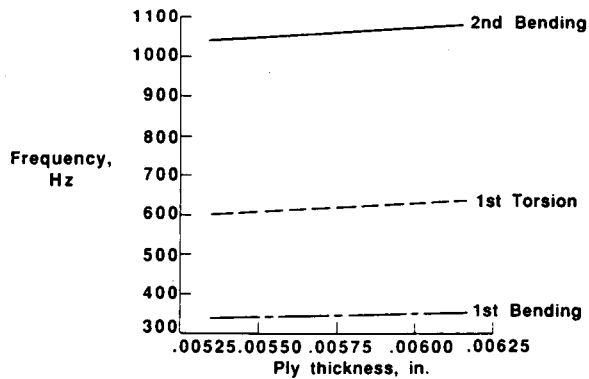
7

Fig. 12 - Modal frequency as a function of ply thickness

Conclusions

Dynamic finite-element analyses of a composite tube exhibiting extension-twist elastic coupling have been conducted and compared with experimental test data. Because the composite tube specimen possessed a significant amount of permanently-affixed non-structural mass, four mass representation studies were performed to determine the most favorable mass modeling configuration for the tube. The modeling configuration in which the primary components of the non-structural mass (aluminum end plugs and potting compound) were modeled as a single mass with the respective inertial properties produced good agreement with experimental frequency data (maximum error of 13.4%) , and was therefore selected as the baseline model. An analysis using a simplified beam finite-element representation of the specimen with the equivalent engineering stiffnesses was also performed. Results from this "equivalent-beam" analysis were compared with those obtained from the baseline finite-element model as well as experimental data. This comparison was performed to establish the range of applicability of the simpler beam analysis. Results indicated that, although the equivalent-beam analysis yielded accurate frequencies for the bending modes, an appreciable degradation in the torsional frequency prediction was evident, due to the absence of off-diagonal coupling terms in the formulation of the equivalent engineering stiffnesses. In addition, parametric studies of frequency variation were performed on a simplified version of the baseline finite-element model to assess the effects of ply orientation angle and ply thickness. The results of the ply orientation study indicated an essentially linear response in frequency variation for small perturbations of the ply angle. For each 1° increment in ply angle, the first and second bending frequencies varied inversely with ply angle an average of 1.8%, as compared to the torsional frequency, which varied directly with ply angle an average of 1.5%. However, modal frequencies were only slightly sensitive to small perturbations in ply thicknesses. While essentially linear trends were again noted, the average variations in bending and torsional frequencies were diminished (approximately a 0.4% variation in bending frequencies, and 0.8% variation in torsional frequency, per 0.0001 inch variation in ply thickness).

References

1. Dong, Stanley B.: Free Vibration of Laminated Orthotropic Cylindrical Shells, *Journal of the Acoustical Society of America*, Vol. 44, (6), 1968.

2. Sharma, C.B., and Darvizeh, M.: Calculation of Natural Frequencies of Specially Orthotropic Multi-Layered Thin Circular Cylinders, *Proceedings of Second International Conference on Recent Advances in Structural Dynamics*, Vol. 1, pp. 15-24, April 1984.

3. Bert, C.W.; Baker, J.L.; and Egle, D.M.: Free Vibrations of Multilayer Anisotropic Cylindrical Shells, *Journal of Composite Materials*, Vol. 3, pg. 480, July 1969.

4. Panda, B., and Chopra, I.: Dynamics of Composite Rotor Blades in Forward Flight, *Vertica*, Vol. 11, No. 112, pp. 187-209, 1987.

5. Hong, C.H., and Chopra, I.: Aeroelastic Stability Analysis of a Composite Bearingless Rotor Blade, *Proceedings of AIAA Structural Dynamics and Materials Conference*, Monterey, CA, April 1987.

6. Stemple, A.D., and Lee, S.W.: A Finite Element Model for Composite Beams with Arbitrary Cross-Sectional Warping, *Proceedings of AIAA Structural Dynamics and Materials Conference*, Monterey, CA, April 1987.

7. Mansfield, E.H., and Sobey, A.J.: The Fibre Composite Helicopter Blade, *Aeronautical Quarterly*, pp. 413-449, May 1979.

8. Bauchau, O.A.: A Beam Theory for Anisotropic Materials, *Journal of Applied Mechanics*, Vol. 52, pp. 416-422, June 1985.

9. Rehfield, L.W.: Design Analysis Methodology for Composite Rotor Blades, *Proceedings of the Seventh DoD/NASA Conference on Fibrous Composites in Structural Design*, June 1985.

10. Gockel, M.A., ed.: *MSC/NASTRAN Handbook for Dynamic Analysis - MSC/NASTRAN Version 63*. MSR-64, MacNeal-Schwendler Corp., June 1983.

11. Schaeffer, H.G.: *MSC/NASTRAN Primer: Static and Normal Modes Analysis*, Milford, NH, Wallace Press, Inc., 1984.

12. Joseph, Jerrard A., ed.: *MSC/NASTRAN Application Manual - CDC Edition*, Vols. 1 and 2, MSR-35 (CDC), MacNeal-Schwendler Corp., August/September and October, 1986.

13. *MSC/NASTRAN User's Manual – MSC/NASTRAN Version 64.* MSR-39, MacNeal-Schwendler Corp., July 1984.

14. *The NASTRAN User's Manual*, Computer Software Management and Information Center (COSMIC), University of Georgia, April 1987 Release.

15. Whetstone, W.D.: *EISI – EAL Engineering Analysis Language Reference Manual*, Vols. 1 and 2, Engineering Information Systems, Inc., July 1983.

16. Rao, K.P.: A Rectangular Laminated Anisotropic Shallow Thin Shell Finite Element, *Computer Methods in Applied Mechanics and Engineering*, 15, pp. 15-33, 1978.

17. Chao, W.C., and Reddy, J.N.: Analysis of Laminated Composite Shells Using a Degenerated 3-D Element, *International Journal for Numerical Methods in Engineering*, Vol. 20, pp. 1991-2007, 1984.

18. Chang, T.Y., and Sawamiphakdi, K.: Large Deformation Analysis of Laminated Shells By Finite Element Method, *Computers and Structures*, Vol. 13, pp. 331-340, 1981.

19. Mau, S.T.; Tong, P.; and Pian, T.H.H.: Finite Element Solutions for Laminated Thick Plates, *Journal of Composite Materials*, Vol. 6, pp. 304-311, April 1972.

20. Panda, S.C., and Natarajan, R.: Finite Element Analysis of Laminated Composite Plates, *International Journal for Numerical Methods in Engineering*, Vol. 14, pp. 69-79, 1979.

21. Hodges, R.H.; Nixon, M.W.; and Rehfield, L.W.: Comparison of Composite Rotor Models: A Coupled-Beam Analysis and an MSC/NASTRAN Finite Element Model, *NASA TM-89024, AVSCOM TM-87-B-2*, February 1987.

Standard Bibliographic Page

1. Report No. NASA TM-100559 AVSCOM TM-88-B-001	2. Government Accession No.	3. Recipient's Catalog No.
4. Title and Subtitle A Preliminary Investigation of Finite-Element Modeling for Composite Rotor Blades		5. Report Date January 1988
		6. Performing Organization Code
7. Author(s) Renee C. Lake and Mark W. Nixon		8. Performing Organization Report No.
9. Performing Organization Name and Address Aerostructures Directorate USAARTA-AVSCOM NASA Langley Research Center Hampton, VA 23665-5225		10. Work Unit No. 505-63-51-01
		11. Contract or Grant No.
12. Sponsoring Agency Name and Address National Aeronautics and Space Administration Washington, D.C. 20546-0001 and U.S. Army Aviation Systems Command St. Louis, MO 63120-1798		13. Type of Report and Period Covered Technical Memorandum
		14. Sponsoring Agency Code

15. Supplementary Notes

Renee C. Lake and Mark W. Nixon: Aerostructures Directorate, USAARTA-AVSCOM

16. Abstract

The results from an initial phase of an in-house study aimed at improving the dynamic and aerodynamic characteristics of composite rotor blades through the use of elastic couplings are presented. Large degree-of-freedom shell-finite-element models of an extension-twist-coupled composite tube were developed and analyzed using MSC/NASTRAN. An analysis employing a simplified beam-finite-element representation of the specimen with the equivalent engineering stiffnesses (equivalent-beam analysis) was additionally performed. Results from the shell-finite-element normal modes and frequency analysis were compared to those obtained experimentally, showing agreement within 13%. In addition, a comparison with results from the equivalent-beam analysis indicated that, although the analysis accurately predicted frequencies for the bending modes, which are essentially uncoupled, there was an appreciable degradation in the frequency prediction for the torsional mode, which is elastically-coupled. This was due to the absence of off-diagonal coupling terms in the formulation of the equivalent engineering stiffnesses. Parametric studies of frequency variation due to small changes in ply orientation angle and ply thickness were also performed. Results showed linear frequency variations less than 2.0% per 1^0 variation in the ply orientation angle, and 1.0% per 0.0001 inch variation in the ply thickness.

17. Key Words (Suggested by Authors(s)) Anisotropy Composite materials Dynamic structural analysis Elastic tailoring Extension-twist coupling Finite-element analysis	18. Distribution Statement Unclassified -- Unlimited Subject Category 39

19. Security Classif.(of this report) Unclassified	20. Security Classif.(of this page) Unclassified	21. No. of Pages 10	22. Price A02

For sale by the National Technical Information Service, Springfield, Virginia 22161